ACS OMEGA

Article

Cite This: ACS Omega 2019, 4, 3188−3197

http://pubs.acs.org/journal/acsodf

# Polyethyleneimine-Modified UiO-66-$NH_2$(Zr) Metal−Organic Frameworks: Preparation and Enhanced $CO_2$ Selective Adsorption

Junjie Zhu, Linbo Wu,* Zhiyang Bu, Suyun Jie,* and Bo-Geng Li

State Key Laboratory of Chemical Engineering at ZJU, College of Chemical and Biological Engineering, Zhejiang University, Hangzhou 310027, China

Supporting Information

**ABSTRACT:** UiO-66-$NH_2$, a zirconium-based functional metal−organic framework (MOF), was postsynthetically modified via Schiff base reaction between aldehyde groups in glutaraldehyde and amino groups in UiO-66-$NH_2$ and $CO_2$-preabsorbed polyethyleneimine (PEI). The resulting PEI-modified MOFs, abbreviated as PEI$^C$@UiO, were characterized with $^1$H NMR, Fourier transform infrared, powder X-ray diffraction, Brunauer−Emmett−Teller, scanning electron microscopy, and thermogravimetric analysis and evaluated as $CO_2$ adsorbents. In comparison with pristine UiO-66-$NH_2$, the PEI$^C$@UiO adsorbents have reduced specific surface area (7−150 $m^2$/g) but maintained the same crystal structure. Particularly, the PEI$^C$96@UiO adsorbent exhibited significantly improved $CO_2/N_2$ adsorption selectivity (48 vs 25) and higher $CO_2$ adsorption capacity (3.2 vs 2.7 mmol/g). The adsorbent also displayed moderate desorption energy (68 kJ/mol $CO_2$), superior moisture endurance, and recyclability, which are very desirable for practical applications.

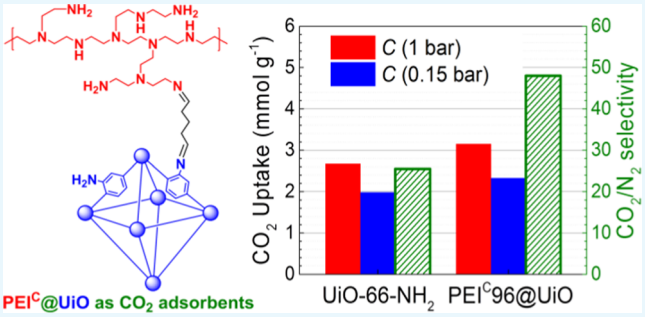


## 1. INTRODUCTION

To control the concentration of carbon dioxide ($CO_2$) in the air, carbon capture, utilization, and storage have received extensive attention in recent years.[1−3] Currently, the chemical absorption using aqueous organic amines like monoethanolamine as absorbent is the most important method for $CO_2$ capture from industrial waste gases.[4−6] However, some inherent drawbacks such as degradation or volatilization of organic amines, equipment corrosion, and high energy consumption limit its practical application. Therefore, various kinds of solid porous adsorbents have been proposed for $CO_2$ capture.

Metal−organic frameworks (MOFs) are three-dimensional porous crystalline materials made up of metal ions or clusters coordinated to organic linkers.[7−10] As a new type of promising adsorbent materials,[11,12] MOFs have shown enormous potential for $CO_2$ capture due to large specific surface area, high crystallinity, tunable chemical structure, and pore properties.[8] However, it remains a challenge to design MOFs with quite high selectivity as well as $CO_2$ adsorption capacity because most MOFs do not possess high $CO_2$ adsorption selectivity. Therefore, much research has been done to improve the $CO_2$ adsorption selectivity of MOFs, including incorporation of open metal sites,[13] construction of size/shape with specific pores,[14] ligand functionalization to introduce strongly polar functional groups,[15] and amine grafting.[16]

As a zirconium(IV)-based MOF, UiO-66 has attracted great interest because of its superior thermal and chemical stability.[17] By functionalizing the ligand of UiO-66 with polar groups such as −$NH_2$, −Br, −$NO_2$, −$(CF_3)_2$, −$SO_3H$, and −$CO_2H$,[18−20] the $CO_2$ adsorption selectivity was improved while retaining the stability, especially when amino group was used as the functional group.[20] Cmarik et al. reported that UiO-66-$NH_2$ showed enhanced $CO_2$ adsorption capacity (2.98 vs 1.75 mmol/g) and adsorption selectivity over $N_2$ (13.2 vs 12.5) at 298 K and 1 bar[20] when compared with UiO-66. The selectivity obtained by applying ideal adsorption solution theory (IAST) for a 15:85 $CO_2/N_2$ gas mixture was 52.[20] Higher $CO_2$ adsorption capacity (3,[21] 3.5[22] mmol/g) and $CO_2/N_2$ selectivity (31[21]) of UiO-66-$NH_2$ were reported by Molavi et al.[21] and Huang et al.[22] Improvement of $CO_2$ capture performance of UiO-66 by polyethyleneimine (PEI) impregnation[23] or ethanolamine grafting[24] was also reported.

For UiO-66-$NH_2$, postsynthetic modification can further improve the $CO_2$ capture performance.[21,25,26] Molavi et al. modified UiO-66-$NH_2$ with glycidyl methacrylate (GMA) by epoxy-amino reaction, resulting in improvement in $CO_2$ adsorption capacity from 3.0 to 4.3 mmol/g and $CO_2/N_2$ selectivity from 31 to 46.[21] The resulting GMA-UiO-66 was further functionalized with ethylenediamine through aza-Michael addition reaction to improve $CO_2$ adsorption capacity up to 5.0 mmol/g.[25] Piperazine-grafted UiO-66-$NH_2$ was reported to have IAST selectivity up to 19 for a 15:85 $CO_2/CH_4$ gas mixture at 298 K at the expense of lower $CO_2$

Received: September 9, 2018
Accepted: January 30, 2019
Published: February 13, 2019




DOI: 10.1021/acsomega.8b02319
ACS Omega 2019, 4, 3188−3197

**Scheme 1. Schematic Diagram for the Synthesis and Hypothesized Structure of the PEI-Modified UiO-66-$NH_2$ Adsorbents ($PEI^C$@UiO)**

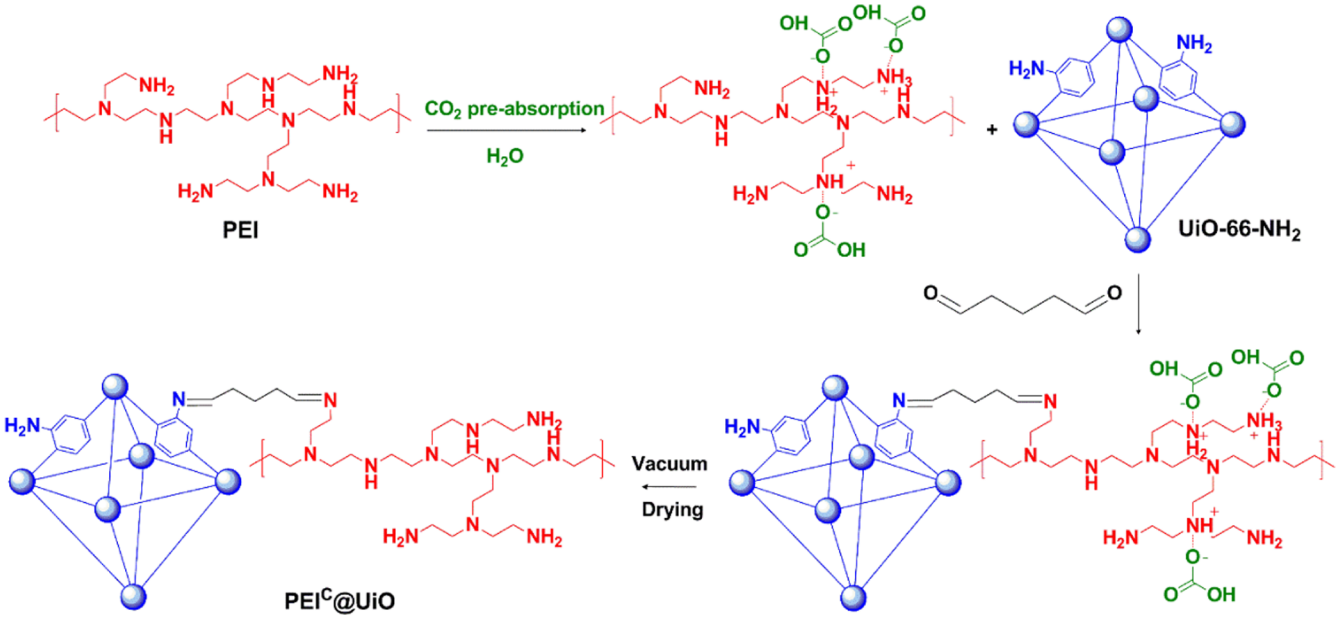


**Table 1. Preparation Conditions and Results of Pristine and PEI-Modified UiO-66-$NH_2$**

| sample | $PEI_{theo}$ [a] (wt %) | $PEI_{theo}$ [b] (wt %) | $W$ [c] (wt %) | $N$ [d] (wt %) | $PEI_{exp}$ [e] (wt %) | $A_p$ [f] ($m^2$/g) | $V_p$ [f] ($cm^3$/g) | $D_p$ [f] (nm) |
|---|---|---|---|---|---|---|---|---|
| UiO-66-$NH_2$ | 0 | 0 | 0 | 5.0 | 0 | 987 | 0.51 | 2.05 |
| $PEI^C$48@UiO | 48 | 26 | 41 | 6.8 | 10.6 | 151 | 0.14 | 3.58 |
| $PEI^C$72@UiO | 72 | 34 | 64 | 9.0 | 19.4 | 12.0 | 0.076 | 25.4 |
| $PEI^C$96@UiO | 96 | 41 | 90 | 9.5 | 22.4 | 7.64 | 0.11 | 55.5 |
| PEI72@UiO | 72 | 34 | 62 | 8.4 | 17.3 | 14.4 | 0.096 | 26.5 |
| PEI96+UiO | 96 | 49 | 89 | 16.0 | 43.4 | 1.40 | 0.0034 | 9.60 |

[a]The mass percentage of PEI used in adsorbent synthesis, based on the mass of UiO-66-$NH_2$. [b]The mass percentage of PEI used in adsorbent synthesis, based on the sum of UiO-66-$NH_2$, PEI, and GD fed. [c]Weight gain based on the mass of UiO-66-$NH_2$, calculated from the weight change before and after the modification reaction. [d]Nitrogen content measured by elemental analysis. [e]PEI content in adsorbent, calculated by nitrogen content. [f]$A_p$: specific surface area; $V_p$: total pore volume; $D_p$: average pore size.

adsorption capacity.[26] Interaction between amines with the open metal sites of MOFs has also been reported to improve $CO_2$ adsorption capacity of MOFs at low pressure and room temperature, such as *N,N′*-dimethylethylenediamine (mmen)/[$Mg_2$(dobpdc)],[27] ethylenediamine/ZIF-8,[28] tetraethylenepentamine (TEPA)/MIL-101-$NH_2$,[29] polyethyleneimine (PEI)/MIL-101,[30,31] PEI/MIL-101-$NH_2$,[3232] and PEI/HKUST[33] composites. In all these amine-modified MOFs, the MOFs act as supports with large specific surface area and the amine groups adsorb $CO_2$. The synergism between them results in enhancement of the $CO_2$ adsorption capacity and selectivity. PEI is a suitable polyamine with highly dense amine groups, especially accessible primary amine sites at chain ends, which can react with $CO_2$ by forming carbamates.[34] But as a viscous liquid, PEI itself is not a suitable candidate for $CO_2$ adsorption. Therefore, PEI is usually supported onto porous materials such as zeolites,[35] microporous/mesoporous silica,[36] and porous polymers[37] as well as MOFs[23,30−33] to improve their $CO_2$ sorption. Because of the higher porosity and specific surface area, MOFs seems to be more suitable for PEI incorporation to reach high $CO_2$ adsorption capacity.

In this work, we report PEI-modified UiO-66-$NH_2$ in an attempt to prepare $CO_2$ adsorbent with high adsorption capacity, kinetics, and selectivity. UiO-66-$NH_2$ was post-synthetically modified with PEI in the presence of glutaraldehyde (GD) via Schiff base reaction. The adsorbents were characterized with $^1$H NMR, Fourier transform infrared (FTIR), powder X-ray diffraction (PXRD), scanning electron microscopy (SEM), and thermogravimetric analysis (TGA). $CO_2$ adsorption was tested under different conditions to evaluate the adsorbents for potential application in $CO_2$ capture from flue gas.

## 2. RESULTS AND DISCUSSION

**2.1. Synthesis and Structural Characterization.** Powdery UiO-66-$NH_2$ was prepared according to a previously reported procedure and then postsynthetically modified with PEI in the presence of GD, which linked UiO-66-$NH_2$ and PEI together through Schiff base reaction, as illustrated in Scheme 1. He et al.[42] reported that a $CO_2$-imprinted solid amine adsorbent prepared by cross-linking $CO_2$-preabsorbed PEI with glutaraldehyde showed a 25% higher $CO_2$ adsorption capacity. In this study, $CO_2$-preabsorbed PEI was also used in the postsynthetic modification to prepare three adsorbents named as $PEI^C$@UiO*x*, in which *x* (48, 72, and 96%) means mass percentage of PEI based on UiO-66-$NH_2$. For comparison, PEI72@UiO was prepared using PEI without $CO_2$ preabsorption and PEI96+UiO was prepared by impregnation of PEI in the absence of glutaraldehyde. Detailed



DOI: 10.1021/acsomega.8b02319
ACS Omega 2019, 4, 3188−3197

preparation conditions and structural characteristics of the adsorbents are summarized in Table 1. The PEI content in the adsorbent ($PEI_{exp}$) was calculated by the following formula

$$PEI_{exp} = \frac{(1 + W) \times N - N(\text{UiO-66-NH}_2)}{N(\text{PEI}) \times (1 + W)}$$

where $W$ is the weight gain based on the unit mass of UiO-66-$NH_2$, $N$ is the nitrogen content of the adsorbent measured by elemental analysis, and $N$(PEI) is the theoretical nitrogen content (30.74 wt %) of PEI. For the three PEI$^C$@UiO samples, PEI content (10.6−22.4 wt %) increased with increasing PEI feeding (48−96 wt %) while the color changes from yellow to grayish brown. The weight gain is less than the PEI feeding for all the samples. It seems to be independent of $CO_2$ preabsorbing PEI (PEI$^C$72@UiO vs PEI72@UiO) or the presence of glutaraldehyde (PEI$^C$96@UiO vs PEI96+UiO). But, the nitrogen content of PEI96+UiO is clearly higher than that of PEI$^C$96@UiO because both PEI and nitrogen-free glutaraldehyde are gained in PEI$^C$96@UiO but only PEI is gained in PEI96+UiO. From these results, it is concluded that only partial PEI has been incorporated onto the surface of the MOF, especially in the chemically modified PEI@UiO and PEI$^C$@UiO series. The incomplete chemical grafting of PEI may be attributed to the steric hindrance imposed by partial pendant $-NH_2$ groups, which point to the MOF cavities other than those outside.[38] In other words, these $-NH_2$ groups in the MOF did not contribute to graft PEI. Another possibility is that partial glutaraldehyde reacted with the MOF or PEI itself, resulting in intra-cross-linking of MOF or PEI instead of PEI grafting onto the MOF.

Figure 1 shows the $^1$H NMR spectra of PEI-modified and PEI-impregnated UiO-66-$NH_2$ adsorbents after digestion in

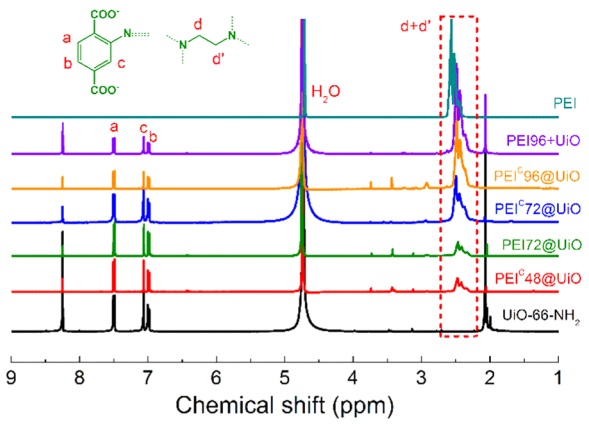


**Figure 1.** $^1$H NMR spectra of PEI, UiO-66-$NH_2$, and PEI-modified MOFs. The samples except PEI were digested for 24 h in a 1 M solution of NaOH/$D_2O$ before NMR measurement.

NaOH/$D_2O$ solution as well as PEI itself. In UiO-66-$NH_2$, as expected, the three proton signals of 7.02, 7.09, and 7.53 ppm are attributed to the benzene ring structure (3 × 1H) of organic ligand in MOFs. The peak at 2.07 ppm is attributed to Zr−OH[43] formed during digestion. The reason of the peak at 8.27 ppm is not clear yet. It also exists in the spectrum of digested UiO-66-$NH_2$ reported previously.[44] After PEI modification, the multiple broad proton signals of $-CH_2$ in PEI and glutaraldehyde appeared at 2.3−2.6 ppm. The peak intensity shows an increasing trend while the PEI loading increased. However, −N═CH bond formatted by Schiff base reaction of glutaraldehyde was not observed in PEI@UiO & PEI$^C$@UiO. It was possible that −N═CH bonds were unstable under alkaline conditions and ruptured.

The FTIR spectra shown in Figure 2 provided more information for the products. For UiO-66-$NH_2$, a strong peak

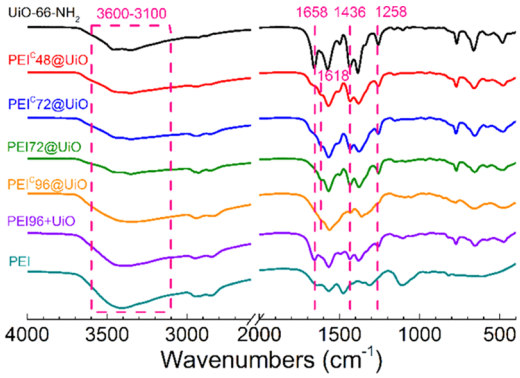


**Figure 2.** FTIR spectra of PEI, UiO-66-$NH_2$, and PEI-modified MOFs.

at 1658 $cm^{-1}$, assigned to the $\nu$(C═O) stretching of *N*,*N*-dimethylformamide (DMF) can be seen. The absence of this band in PEI$^C$@UiO-66 indicates the complete exchange of DMF with water.[45] The 3000−2800 and 3600−3100 $cm^{-1}$ signals are assigned to the stretching vibration of $CH_2$ and unreacted amino groups, respectively. They became stronger when more PEI was incorporated. The characteristic stretching vibration peaks of $NH_2$ on the MOF appeared at 1436 and 1258 $cm^{-1}$. The two peaks were weakened because of its Schiff base reaction with aldehyde group in glutaraldehyde to form N═C bond at 1618 $cm^{-1}$ (stretching vibration), resulting PEI grafting shown in Scheme 1. In addition to the grafting reaction, the intra-cross-linking reactions of PEI and UiO-66-$NH_2$ with glutaraldehyde also occurred unavoidably at the same time. In fact, all these Schiff base reactions contributed to the signal at 1618 $cm^{-1}$, but could not be identified from each other in the FTIR results. For simplicity and clarity, Scheme 1 only shows the expected grafting structure of the products.

The PXRD patterns of UiO-66-$NH_2$ and the five PEI-modified adsorbents are shown in Figure 3. The as-synthesized UiO-66-$NH_2$ showed narrow diffraction peaks in accordance with previously published data,[17,38] confirming successful synthesis and high crystallinity of UiO-66-$NH_2$. The PXRD patterns of PEI-modified MOFs were essentially identical to

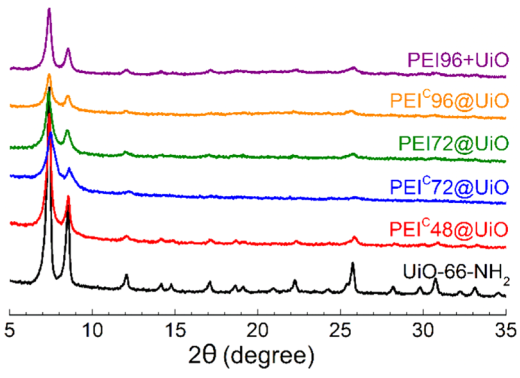


**Figure 3.** Powder X-ray diffraction (PXRD) patterns of pristine UiO-66-$NH_2$ and PEI-modified adsorbents.



DOI: 10.1021/acsomega.8b02319
ACS Omega 2019, 4, 3188−3197

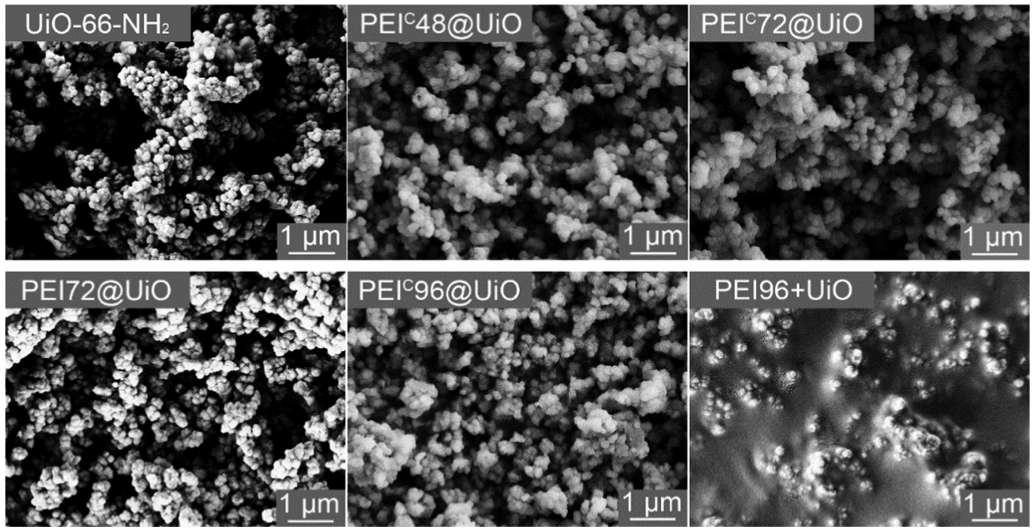


**Figure 4.** SEM images of pristine UiO-66-$NH_2$ and PEI-modified adsorbents.

that for the parent UiO-66-$NH_2$, indicating that the crystal structure of UiO-66-$NH_2$ was well maintained after the modification. The peak intensity of UiO-66-$NH_2$ decreased after PEI modification because of the decrease of MOF content and the enhancement of the interaction between the PEI amino groups and the UiO-66-$NH_2$ Zr sites.[23] Another reason that cannot be completely excluded is that the MOF framework structure could be destroyed to some extent in alkali amine solution though UiO-66-$NH_2$ is reported to show excellent alkali resistance.[38] Similar structure destruction were reported in some amine-impregnated MOFs, such as MIL-101,[31] HKUST-1,[33] and MOF-74.[46]

The nitrogen adsorption isotherms of the five PEI-modified adsorbents and UiO-66-$NH_2$ are shown in Figure S1. The specific surface areas calculated from $N_2$ adsorption isotherms are listed in Table 1. It reaches 987 $m^2/g$ for UiO-66-$NH_2$ but decreases to 151, 12.0, and 7.6 $m^2/g$ for PEI$^C$48@UiO, PEI$^C$72@UiO, and PEI$^C$96@UiO, respectively. At the same time, the average pore size gradually increases and the pore volume decreases with increasing PEI loading. The results suggested that PEI modification remarkably decreased the specific surface area of UiO-66-$NH_2$ due to the pore-filling effect of PEI on the macropores between MOF particles. Whether or not pretreating PEI with $CO_2$ preabsorption did not show clear influence on the pore characteristics (PEI$^C$72@UiO vs PEI72@UiO), but impregnation of UiO-66-$NH_2$ with large amount of PEI (PEI96+UiO) led to serious pore blockage (supported by SEM observation, see next paragraph), making the micropores in MOF crystals no longer accessible for $N_2$ adsorption. Therefore, PEI96+UiO only maintained a very small surface area of 1.40 $m^2/g$.

To further understand the effect of PEI modification on the pore characteristic, the morphological structure of the samples was further observed by SEM. As shown in Figure 4, the UiO-66-$NH_2$ appears to be near-spherical crystals. For PEI@UiO or PEI$^C$@UiO series, the morphology of MOF particles did not show an observable change though there might exist PEI in the intercrystal void of UiO-66-$NH_2$. But for PEI96+UiO, the surface and intercrystal void of UiO-66-$NH_2$ crystals are almost fully occupied by PEI. In other words, the UiO-66-$NH_2$ crystals are embedded in the PEI layers. This phenomenon explains why the specific surface area of PEI96+UiO was very low.

$CO_2$ adsorbents must have enough thermal stability to endure high temperature of at least 100−150 °C of flue gas.[47] The TGA curves of UiO-66-$NH_2$ and the five PEI-modified adsorbents are shown in Figure 5. The TGA curves of UiO-66-$NH_2$ showed a two-step weight loss. The initial weight loss at 100−280 °C was ascribed to the removal of adsorbed gas and dehydroxylating of the zirconium oxoclusters.[38] The second-step weight loss (after 280 °C) was due to the framework decomposition.[38] The PEI-modified adsorbents were all stable up to 200 °C, if we ignore the initial weight loss over 100 °C, which possibly results from absorbed water and gases. At temperature higher than 200 °C, the weight loss was caused mainly by PEI decomposition. With the increase of PEI loading, the weight loss curve moves toward low temperature side. The differences in preparation methods do not show a clear influence on thermal stability. In conclusion, the PEI-modified adsorbents have good thermal stability to endure normal flue gas temperature for $CO_2$ separation.

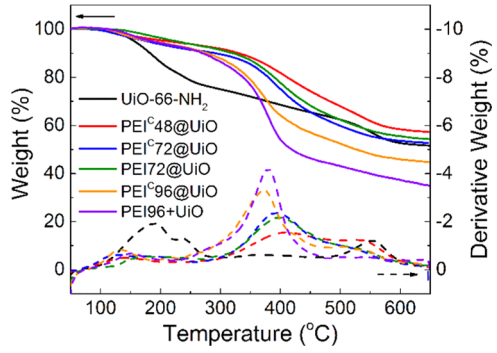


**Figure 5.** TGA curves of pristine UiO-66-$NH_2$ and PEI-modified adsorbents ($N_2$ atmosphere, heating rate 10 °C/min).

**2.2. $CO_2$ Adsorption Capacity, Rate, and Selectivity over $N_2$.** $CO_2$ adsorption performance of UiO-66-$NH_2$ and the five PEI-modified adsorbents at 25 °C and 1 atm is shown in Figure 6A. The saturated adsorption capacity of UiO-66-$NH_2$ reaches up to 2.67 mmol $CO_2/g$. It is roughly in accordance with some of the reported values (2.86−3.15 mmol



DOI: 10.1021/acsomega.8b02319
ACS Omega 2019, 4, 3188−3197

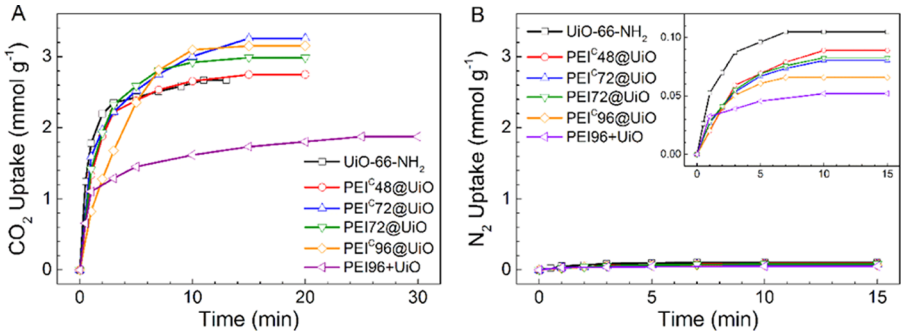


**Figure 6.** $CO_2$ (A) and $N_2$ (B) adsorption behaviors of pristine UiO-66-$NH_2$ and PEI-modified adsorbents.

**Table 2. $CO_2$ Adsorption/Desorption Properties of Pristine UiO-66-$NH_2$ and PEI-Modified Adsorbents**

| | $C_{s,1bar}$[a] (mmol $CO_2$/g) | | | | | |
|---|---|---|---|---|---|---|
| adsorbent | dry | moist[b] | $\alpha$ | $C_{s,exp}$[c] (mmol $CO_2$ + $N_2$/g) | $C_{s,0.15bar}$[d] (mmol $CO_2$/g) | $Q_{des}$[e] (kJ/mol $CO_2$) |
| UiO-66-$NH_2$ | 2.67 | 2.13 | 25.5 | 2.06 | 1.98 | |
| PEI[C]48@UiO | 2.75 | 2.69 | 30.9 | 2.06 | 2.00 | 63.3 |
| PEI[C]72@UiO | 3.26 | 3.43 | 40.6 | 2.17 | 2.12 | 67.3 |
| PEI72@UiO | 2.99 | 3.02 | 36.1 | 2.10 | 2.04 | |
| PEI[C]96@UiO | 3.15 | 3.33 | 48.0 | 2.38 | 2.33 | 68.0 |
| PEI96+UiO | 1.87 | 2.69 | 36.0 | 1.59 | 1.55 | |

[a]Experimental $CO_2$ adsorption capacity. [b]The $CO_2$ adsorption capacity measured with moist $CO_2$. [c]Experimental gas adsorption capacity measured in simulated flue gas (14.3 vol % $CO_2$). [d]$CO_2$ adsorption capacity calibrated by the separation factor $\alpha$ in simulated flue gas. [e]The $CO_2$ desorption heat.

$CO_2$/g).[21] In comparison, the PEI[C]@UiO adsorbents exhibit higher adsorption capacity ranging from 2.75 to 3.26 mmol $CO_2$/g (Table 2). The $NH_2$ groups in PEI and UiO-66-$NH_2$ contributed to chemical $CO_2$ adsorption, and the pores in UiO-66-$NH_2$ contributed to physical $CO_2$ adsorption. However, partial $NH_2$ groups in UiO-66-$NH_2$ that had converted to N═C bonds no longer contributed to $CO_2$ adsorption and offset part of the contribution of PEI to $CO_2$ adsorption. The amount of incorporated PEI is not positively correlated with the $CO_2$ adsorption capacity. Among them, PEI[C]72@UiO shows the highest adsorption capacity, 3.26 mmol $CO_2$/g. In comparison with PEI72@UiO, PEI[C]72@UiO shows 9% higher $CO_2$ adsorption capacity (3.26 vs 2.99 mmol $CO_2$/g). The increment is higher than the experimental error (<3%) but not as high as the value (25%) reported previously.[42] The saturated adsorption capacity of PEI96+UiO is much lower than that of PEI[C]96@UiO (1.87 vs 3.15 mmol $CO_2$/g) because of its much lower specific surface area.

Furthermore, it can be seen that all the PEI@UiO adsorbents exhibit high adsorption rate, reaching saturated adsorption capacity in 15 min. However, PEI96+UiO need much longer time to reach $CO_2$ saturation due to low specific surface area and consequent slower adsorption rate.

$CO_2/N_2$ adsorption selectivity is another important indicator to evaluate a solid sorbent for practical use. For this purpose, the adsorption of pure $N_2$ (60 mL/min) was conducted under the same condition. The results are shown in Figure 6B and listed in Table 2. UiO-66-$NH_2$ adsorbed $N_2$ significantly (0.11 mmol/g). But, the PEI[C]@UiO adsorbents had a relatively small amount of $N_2$ adsorption, decreasing to 0.06−0.09 mmol/g. The separation factor $\alpha$ (adsorption selectivity of $CO_2$ over $N_2$) was calculated by the formula

$$\alpha = \frac{Q_{CO_2}/P_{CO_2}}{Q_{N_2}/P_{N_2}}$$

where $Q_i$ and $P_i$ ($P_i$ = 1 bar here) are the adsorption capacity and the partial pressure of component $i$, respectively. The separation factor of UiO-66-$NH_2$ is 25.5, which is between the reported values in literature (13[20]−32[21]). After PEI modification, the value of PEI[C]@UiO increased to 30.9−48.0. As expected, it was obviously improved with increasing PEI loading.

To simulate flue gas that usually contains about 15 vol % $CO_2$, a $CO_2/N_2$ mixture gas (10 + 60 mL/min, $CO_2$ 14.3 vol %) was also used for $CO_2$ adsorption. The result is shown in Figure 7. The saturated gas adsorption capacity of PEI[C]@UiO was 2.06−2.38 mmol $CO_2$ + $N_2$/g. The true $CO_2$ sorption capacity from the mixed gas ($C_{s,0.15bar}$) can be calibrated by the following formula. The adsorption rate and capacity for simulated flue gas both decreased to some extent in

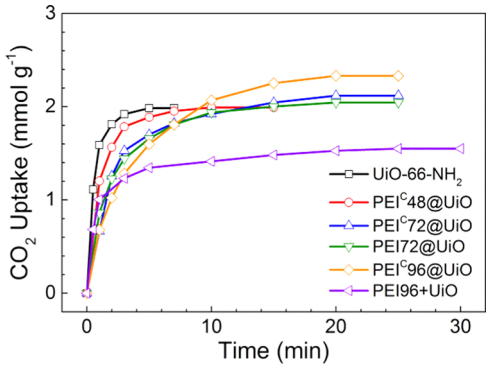


**Figure 7.** $CO_2$ uptake of pristine UiO-66-$NH_2$ and PEI-modified adsorbents from $CO_2$ + $N_2$ mixture containing $CO_2$ 15% at 25 °C.



DOI: 10.1021/acsomega.8b02319
ACS Omega 2019, 4, 3188−3197

Table 3. $CO_2$ Adsorption Performance of Different Adsorbents

| adsorbents[a] | $T^b$ (K) | $C_s^c$ (mmol/g) 1 bar | $C_s^c$ (mmol/g) 0.15 bar | $\alpha^d$ | $\alpha^e$ | refs |
|---|---|---|---|---|---|---|
| $PEI_C$96@UiO | 298 | 3.1 | 2.3 | 48 | | this work |
| PEI (50%) + silica | 348 | 3.1 | 3.0 | | | 36 |
| 0.70PEI@PDVB | 298 | 3.2 | 2.4 | | | 37 |
| PEI@PS polyHIPE | 313 | 3.5 | | 26 | | 49 |
| PEI@poly(GMA)HIPE | 313 | 4.0 | 3.1 | 27 | | 50 |
| PEI + UiO-66 | 298 | 3.3 | 1.6 | | | 23 |
| GMA-UiO-66 | 298 | 4.3 | 1.8 | 46 | | 21 |
| TEPA (50%) + $NH_2$-MIL-101 | 298 | 3.1 | | | | 29 |
| PEI (2.5%) + HKUST | 298 | 4.1 | 0.8 | 2 | | 32 |
| en-[$Mg_2$(dobpdc)] | 298 | 4.5 | 3.5 | | 230 | 16 |
| pyrrolic N-enriched carbon | 298 | 3.6 | 1.5 | | 115 | 51 |

[a]PAF: porous aromatic framework; PDVB: nanoporous poly(divinylbenzene). PS: poly(styrene divinylbenzene), modified with polyacrylic acid. [b]Temperature. [c]$CO_2$ adsorption capacity at the indicated $CO_2$ partial pressure. [d]$CO_2/N_2$ selectivity: $\alpha = nCO_2$ (1 bar)/$nN_2$ (1 bar). [e]Calculated by ideal adsorption solution theory (IAST) model, $\alpha = [nCO_2$ (0.15 bar)/$nN_2$ (0.85 bar)] × (0.85/0.15).

comparison with those for pure $CO_2$[48] due to lower $CO_2$ partial pressure. Among them, $PEI^C$96@UiO reaches the highest adsorption capacity (2.33 mmol $CO_2$/g).

$$C_{s,0.15bar} = C_{s,exp} \times \frac{\alpha}{1+\alpha}$$

The $PEI^C$96@UiO is compared with some other $CO_2$ adsorbents reported in literature. As shown in Table 3, it can be seen that this functional MOF adsorbent shows a reasonably good $CO_2$ adsorption performance, especially in $CO_2$ selectivity.

**2.3. $CO_2$ Desorption Enthalpy.** Differential scanning calorimetry (DSC) was used to determine the $CO_2$ desorption heat ($Q_{des}$). As shown in Figure 8, a strong endotherm (155−191 J/g $CO_2$-saturated adsorbent) was observed for all the three $CO_2$-saturated $PEI^C$@UiO adsorbents due to $CO_2$ desorption but none for the neat $PEI^C$96@UiO. The $CO_2$ desorption occurred in a wide temperature range from 70 to 230 °C, and the endotherm peak temperature appears at 133−144 °C. From the desorption enthalpy value, the desorption heat $Q_{des}$ (kJ/mol $CO_2$) of $CO_2$-saturated $PEI^C$@UiO can be calculated by the equation $Q_{des} = E/(C_s/(C_sM_{CO_2}/1000 + 1))$, where $E$, $C_s$, $M_{CO_2}$ are the desorption enthalpy (J/g), the $CO_2$ adsorption capacity (mmol/g), and the molar mass of $CO_2$ (44 g/mol), respectively. The value ranges from 63.3 to 68.0 kJ/mol $CO_2$, higher than that of pristine UiO-66-$NH_2$ (ca. 27 kJ/mol).[20] The more PEI is incorporated, the higher the $CO_2$ desorption heat is. The values are located in the range of 60−90 kJ/mol of typical chemsorption[47] but lower than the typical value, ca. 80 kJ/mol, of alkanolamine aqueous solution.[52,53] Therefore, this $CO_2$ adsorbent seems competitive in reducing the regeneration energy consumption.

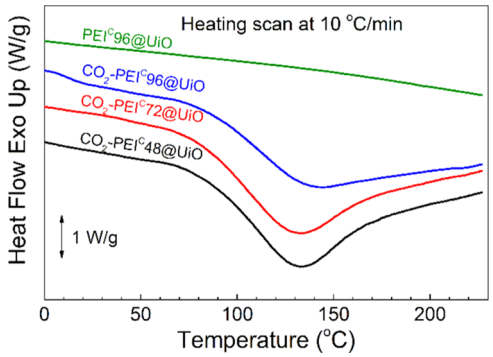


Figure 8. DSC curves of neat $PEI^C$96@UiO and three $CO_2$-saturated $PEI^C$@UiO adsorbents.

**2.4. Effect of Moisture on $CO_2$ Adsorption.** Moisture is a non-negligible factor that affects practical $CO_2$ capture from flue gas, which usually contains 8−17% water vapor.[54] Due to the hydrophilicity, the adsorbents unavoidably adsorb water vapor from the flue gas. To determine the water content in adsorbents during $CO_2$ capture, the water adsorption of $PEI^C$96@UiO at 25 °C was measured. This hygroscopic adsorbent adsorbed 1.7 wt % water in 15 min. To study the influence of moisture on $CO_2$ adsorption, dry $CO_2$ (d-$CO_2$) and moist $CO_2$ (m-$CO_2$) were used to pass through dry adsorbent (d-Sorb) separately. The moist $CO_2$ gas was obtained by feeding dry $CO_2$ gas through water. The results are shown in Figure 9.

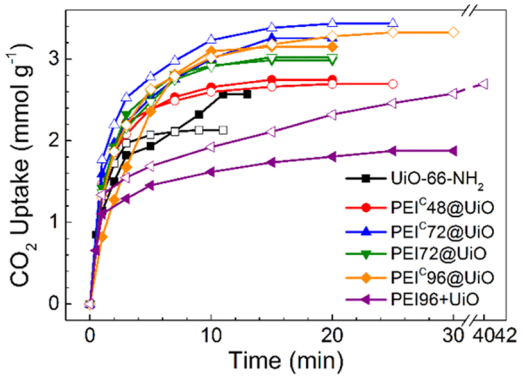


Figure 9. $CO_2$ adsorption of pristine UiO-66-$NH_2$ and PEI-modified adsorbents using dry or moist $CO_2$ gas (solid: d-$CO_2$; hollow: m-$CO_2$).

As hygroscopic adsorbents, UiO-66-$NH_2$ showed a 20.2% decrease in $CO_2$ adsorption capacity in the "m-$CO_2$ + d-Sorb" case because water vapor adsorption competed with $CO_2$ adsorption. The existence of water could also affect the $CO_2$ binding to the open metal sites in MOF.[55] The adsorption capacity of $PEI^C$48@UiO slightly decreased by 2.2%, which was within the allowable error range of the adsorption



DOI: 10.1021/acsomega.8b02319
ACS Omega 2019, 4, 3188−3197

experiment. However, $CO_2$ adsorption capacity of PEI$^C$72@UiO, PEI$^C$96@UiO, and PEI96+UiO increased in the m-$CO_2$ + d-Sorb case by 5.2, 5.7, and 43.8%, respectively. The rise instead of descent in $CO_2$ adsorption is attributed to the tertiary amino groups in PEI (about 12 wt %), which might contribute to $CO_2$ adsorption in the presence of moisture.[56] Therefore, the PEI$^C$@UiO adsorbents show excellent moisture endurance in $CO_2$ adsorption.

**2.5. Adsorption/Desorption Cycles.** Finally, $CO_2$ adsorption/desorption cycles of PEI$^C$96@UiO were conducted to assess the recyclability and durability of the adsorbent. The $CO_2$ desorption was carried out at 120 °C. The same temperature was also used for the $CO_2$ desorption of aqueous monoethanolamine absorbent.[52] Pure $N_2$ purging was used instead of vacuum to facilitate the desorption experiment, though the latter seemed more suitable for practical $CO_2$ capture. Figure 10 shows three cycles of $CO_2$ adsorption/desorption of PEI$^C$96@UiO. Because of weak chemical bonding between PEI$^C$96@UiO and $CO_2$ at high temperature, the adsorbed $CO_2$ was desorbed rapidly and nearly completely. In each cycle, the adsorbent effectively captured 3.0 mmol $CO_2$/g. A high adsorption capacity, 97.4%, was retained after three cycles. The preadsorded moisture and $N_2$ might account for the slight loss in adsorption capacity. In conclusion, PEI$^C$96@UiO, showed quite steady $CO_2$ adsorption and superior durability.

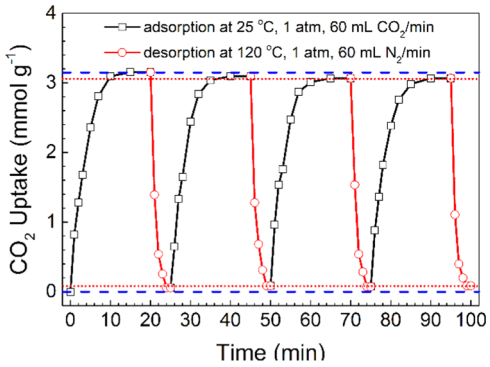


**Figure 10.** $CO_2$ adsorption/desorption cycles of PEI$^C$96@UiO.

## 3. CONCLUSIONS

UiO-66-$NH_2$, a zirconium-based functional metal−organic framework (MOF), was postsynthetically modified with $CO_2$-preabsorbed polyethyleneimine (PEI) via Schiff base reaction. The resulting PEI$^C$@UiO adsorbents contain PEI up to 22.1 wt % or nitrogen up to 9.5 wt %. They show specific surface area of 7−150 $m^2$/g and maintain unchanged crystal structure of the MOF. When compared with pristine UiO-66-$NH_2$, PEI$^C$96@UiO shows significantly improved $CO_2/N_2$ adsorption selectivity (48 vs 25) and higher $CO_2$ adsorption capacity (3.2 vs 2.7 mmol/g), but retains fast $CO_2$ adsorption/desorption in spite of its reduced specific surface area. It also displays moderate desorption heat (68 kJ/mol $CO_2$), superior moisture endurance, and recyclability, which are very desirable for practical applications. Further studies on raising PEI content as well as maintaining high specific surface will be reported elsewhere.

## 4. EXPERIMENTAL SECTION

**4.1. Materials.** Zirconium tetrachloride ($ZrCl_4$, 98%), branched polyethyleneimine (PEI, 99%, $M_w$ = 600, viscous liquid, theoretical amino group content 32.9 wt %, primary amino group content 12.8 wt %), and glutaraldehyde (GD, 50%) were purchased from Aladdin Chemical Co. Ltd. China. 2-Aminobenzene-1,4-dicarboxylic acid (ABDC or $H_2$BDC-$NH_2$, 98%) was supplied by J&K Chemicals. *N*,*N*-dimethylformamide (DMF), anhydrous ethanol, anhydrous methanol, sodium hydroxide (NaOH), and hydrochloric acid (HCl, 36.5%) were all analytical grade reagents purchased from Sinopharm Chem. Reagent Co. Ltd. China. All chemicals were used as received. Nitrogen ($N_2$, ≥99.5%) and carbon dioxide ($CO_2$, ≥99.995%) were obtained from Jingong Specialty Gases Co., Ltd. China.

**4.2. Synthesis of UiO-66-$NH_2$.** [$Zr_6O_4(OH)_4$(BDC-$NH_2$)$_6$] (UiO-66-$NH_2$) was prepared according to a procedure previously reported,[20,38] with some modifications. In brief, $ZrCl_4$ (5 mmol, 1.166 g), DMF (15 mL), and HCl (5 mL) were mixed and sonicated for 20 min until all materials were dissolved fully at room temperature. ABDC (5 mmol, 0.9057 g) and the residual DMF (35 mL) were then added and the mixture was sonicated for another 20 min. The homogeneous mixture was heated at 80 °C for 12 h and then at 100 °C for 24 h. The resulting product precipitated as microcrystalline powder. The mixture was cooled down to room temperature and centrifuged at 8000 rpm for 10 min to separate the solid from the solution. After washing three times with DMF (30 mL) and ethanol (30 mL), respectively, and drying under vacuum at 100 °C for 24 h, yellow powder was finally obtained at a yield of 92%.

**4.3. Synthesis of PEI-Modified UiO-66-$NH_2$ Adsorbent (PEI$^C$@UiO and PEI@UiO).** Scheme 1 depicts the preparation process. PEI (0.375, 0.563, or 0.751 g) was dissolved in water (10.0 mL). $CO_2$ was fed into the resulting solution at room temperature to prepare $CO_2$-preabsorbed PEI. After 2 h, UiO-66-$NH_2$ (0.5 mmol, 0.78 g) was added. After stirring at 400 rpm for 30 min, an aqueous solution of GD (0.6007 g) was added dropwise under stirring at room temperature for another 12 h. The resulting solid was isolated via centrifugation and washed with deionized water three times. After vacuum drying at 100 °C for 24 h to remove absorbed $CO_2$ and solvent, a blocky solid product was obtained. It was symbolized as "PEI$^C$x@UiO", where UiO and superscript C represented UiO-66-$NH_2$ and preabsorption of $CO_2$, x was the mass percentage of PEI fed based on UiO-66-$NH_2$. An adsorbent was also prepared without $CO_2$ preabsorption. In this case, the product was named as "PEIx@UiO". The details of preparation conditions and structural characteristics of the adsorbents are listed in Table 1.

**4.4. Preparation of PEI-Impregnated UiO-66-$NH_2$ Adsorbent (PEI + UiO).** A PEI-impregnated UiO-66-$NH_2$ adsorbent was also prepared using an impregnation method according to the procedure previously reported for PEI-impregnated UiO-66 adsorbent.[23] PEI (1.5 mmol, 0.716 g) was dissolved in 5 mL anhydrous methanol. UiO-66-$NH_2$ (0.5 mmol, 0.78 g) powder was added into the solution and the mixture was treated under ultrasonication for 1 h. Then, it was dried under nitrogen atmosphere at 40 °C for 6 h and further dried under vacuum at 100 °C for 12 h. Finally, the obtained sample was symbolized as PEI96+UiO, where UiO represented


DOI: 10.1021/acsomega.8b02319
ACS Omega 2019, 4, 3188−3197

UiO-66-$NH_2$ and 96 was the mass percentage of PEI fed based on UiO-66-$NH_2$.

**4.5. Characterization.** The samples were characterized by elemental analysis (Flash EA1112, ThermoFinnigan Co.), $^1$H NMR (Bruker AC-80 spectroscopy, 400 MHz, NaOH/$D_2O$ solution), and FTIR (Nicolet 5700). Before $^1$H NMR measurement, the PEI-modified samples (20 mg) were digested with 0.6 mL of a NaOH/$D_2O$ solution (1 M) and allowed to stand for 24 h. After the digestion process, the organic portions of the samples (linkers in the MOF and grafted amines) were dissolved, and the inorganic component of the MOF was converted to zirconium hydroxide, which was separated from the solution by filtration.[38] PEI was directly measured using NaOH/$D_2O$ solution (1 M) as the solvent. The FTIR spectra of PEI-modified samples were recorded using KBr disk samples.

Powder X-ray diffraction (PXRD) pattern was measured using a PANalytical X'Pert X-ray diffraction system (PANalytical Company) using Cu K$\alpha$ radiation (1.54 Å), working at 40 kV and 40 mA.

$N_2$ adsorption−desorption isotherms were recorded with a Quantachrome Autosorb-1-C instrument at 77 K. The specific surface area was estimated with the Brunauer−Emmett−Teller (BET) method and the pore volume was calculated with the desorption branch of the isotherms. The samples were degassed at 100 °C for 24 h before BET analysis.

The morphology was recorded with a scanning electron microscope (SEM, Utral 55, Carl zeiss, Germany) at an acceleration voltage of 1.5 kV, using the samples coated with a thin gold layer.

Thermogravimetric analysis (TGA) was recorded with a Perkin-Elmer instrument Pyris 1 TGA analyser under $N_2$ flow (20 mL/min) from 50 to 650 °C at a heating rate of 10 °C $min^{-1}$.

**4.6. $CO_2$ Capture.** Before $CO_2$ adsorption, about 1.0 g of adsorbent was outgassed under vacuum at 100 °C. $CO_2$ adsorption/desorption was performed under atmospheric pressure, as previously reported.[39,40] Desorption of the adsorbent was conducted under pure $N_2$ (60 mL/min) at a temperature of 120 °C. Some repeated experiments of $CO_2$ adsorption and desorption were done. $CO_2$ desorption heat ($Q_{des}$) was recorded with differential scanning calorimetry (DSC, Q200, TA Instrument).[41] The samples were scanned at a heating rate of 10 °C/min under nitrogen flow.

## ■ ASSOCIATED CONTENT

### Supporting Information

The Supporting Information is available free of charge on the ACS Publications website at DOI: 10.1021/acsomega.8b02319.

$N_2$ adsorption isotherms of pristine UiO-66-$NH_2$ and PEI-modified adsorbents (PDF)

## ■ AUTHOR INFORMATION


### Corresponding Authors

*E-mail: wulinbo@zju.edu.cn. Tel: +86 571 87952631. Fax: +86 571 87951612 (L.W.).

*E-mail: zhujunjie116@163.com (S.J.).

### ORCID

Linbo Wu: 0000-0001-9964-6140


### Notes

The authors declare no competing financial interest.

## ■ ACKNOWLEDGMENTS

This work was supported by the National High Technology Research and Development Program (2015BAC04B0103) and 151 Talents Project of Zhejiang Province. The authors thank Mrs. Li Xu, Mrs. Qun Pu and Mrs. Na Zheng for their assistance on in performing BET, DSC, TGA, and SEM analyses at State Key Laboratory of Chemical Engineering (Zhejiang University).

## ■ REFERENCES


(1) Keith, D. W. Why capture $CO_2$ from the atmosphere? *Science* **2009**, *325*, 1654−1655.

(2) Stauffer, P. H.; Keating, G. N.; Middleton, R. S.; Viswanathan, H. S.; Berchtold, K. A.; Singh, R. P.; Pawar, R. J.; Mancino, A. Greening coal: breakthroughs and challenges in carbon capture and storage. *Environ. Sci. Technol.* **2011**, *45*, 8597−8604.

(3) Jung, H.; Jeon, S.; Jo, D. H.; Huh, J.; Kim, S. H. Effect of crosslinking on the $CO_2$ adsorption of polyethyleneimine-impregnated sorbents. *Chem. Eng. J.* **2017**, *307*, 836−844.

(4) Rochelle, G. T. Amine scrubbing for $CO_2$ capture. *Science* **2009**, *325*, 1652−1654.

(5) Han, C.; Graves, K.; Neathery, J.; Liu, K. Simulation of the energy consumption of $CO_2$ capture by aqueous monoethanolamine in pilot plant. *Energy Environ. Res.* **2011**, *1*, 67−80.

(6) Nittaya, T.; Douglas, P. L.; Croiset, E.; Ricardez-Sandoval, L. A. Dynamic modeling and evaluation of an industrial-scale $CO_2$ capture plant using monoethanolamine absorption processes. *Ind. Eng. Chem. Res.* **2014**, *53*, 11411−11426.

(7) Sumida, K.; Rogow, D. L.; Mason, J. A.; McDonald, T. M.; Bloch, E. D.; Herm, Z. R.; Bae, T. H.; Long, J. R. Carbon dioxide capture in metal-organic frameworks. *Chem. Rev.* **2012**, *112*, 724−781.

(8) Zhang, Z.; Zhao, Y.; Gong, Q.; Li, Z.; Li, J. MOFs for $CO_2$ capture and separation from flue gas mixtures: the effect of multifunctional sites on their adsorption capacity and selectivity. *Chem. Commun.* **2013**, *49*, 653−661.

(9) Wang, Q.; Bai, J.; Lu, Z.; Pan, Y.; You, X. Finely tuning MOFs towards high-performance post-combustion $CO_2$ capture materials. *Chem. Commun.* **2016**, *52*, 443−452.

(10) Li, J. R.; Sculley, J.; Zhou, H. C. Metal-organic frameworks for separations. *Chem. Rev.* **2012**, *112*, 869−932.

(11) Belmabkhout, Y.; Guillerm, V.; Eddaoudi, M. Low concentration $CO_2$ capture using physical adsorbents: are metal-organic frameworks becoming the new benchmark materials? *Chem. Eng. J.* **2016**, *296*, 386−397.

(12) Madden, D. G.; Scott, H. S.; Kumar, A.; Chen, K. J.; Sanii, R.; Bajpai, A.; Lusi, M.; Curtin, T.; Perry, J. J.; Zaworotko, M. J. Flue-gas and direct-air capture of $CO_2$ by porous metal-organic materials. *Philos. Trans. R. Soc., A* **2017**, *375*, No. 20160025.

(13) Britt, D.; Furukawa, H.; Wang, B.; Glover, T. G.; Yaghi, O. M. Highly efficient separation of carbon dioxide by a metal-organic framework replete with open metal sites. *Proc. Natl. Acad. Sci. U.S.A.* **2009**, *106*, 20637−20640.

(14) Deng, H.; Grunder, S.; Cordova, K. E.; Valente, C.; Furukawa, H.; Hmadeh, M.; Gándara, F.; Whalley, A. C.; Liu, Z.; Asahina, S.; et al. Large-pore apertures in a series of metal-organic frameworks. *Science* **2012**, *336*, 1018−1023.

(15) Deng, H.; Doonan, C. J.; Furukawa, H.; Ferreira, R. B.; Towne, J.; Knobler, C. B.; Wang, B.; Yaghi, O. M. Multiple functional groups of varying ratios in metal-organic frameworks. *Science* **2010**, *327*, 846−850.

(16) Lee, W. R.; Sang, Y. H.; Ryu, D. W.; Lim, K. S.; Sang, S. H.; Moon, D.; Choi, J.; Chang, S. H. Diamine-functionalized metal-organic framework: exceptionally high $CO_2$ capacities from ambient air and flue gas, ultrafast $CO_2$ uptake rate, and adsorption mechanism. *Energy Environ. Sci.* **2014**, *7*, 744−751.

(17) Cavka, J. H.; Jakobsen, S.; Olsbye, U.; Guillou, N.; Lamberti, C.; Bordiga, S.; Lillerud, K. P. A new zirconium inorganic building




DOI: 10.1021/acsomega.8b02319
*ACS Omega* 2019, 4, 3188−3197

brick forming metal organic frameworks with exceptional stability. *J. Am. Chem. Soc.* **2008**, *130*, 13850−13851.
(18) Yang, Q.; Wiersum, A. D.; Llewellyn, P. L.; Guillerm, V.; Serre, C.; Maurin, G. Functionalizing porous zirconium terephthalate UiO-66(Zr) for natural gas upgrading: a computational exploration. *Chem. Commun.* **2011**, *47*, 9603−9605.
(19) Kronast, A.; Eckstein, S.; Altenbuchner, P. T.; Hindelang, K.; Vagin, S. I.; Rieger, B. Gated channels and selectivity tuning of $CO_2$ over $N_2$ sorption by post-synthetic modification of a UiO-66-type metal-organic framework. *Chem. - Eur. J.* **2016**, *22*, 12800−12807.
(20) Cmarik, G. E.; Kim, M.; Cohen, S. M.; Walton, K. S. Tuning the adsorption properties of UiO-66 via ligand functionalization. *Langmuir* **2012**, *28*, 15606−15613.
(21) Molavi, H.; Eskandari, A.; Shojaei, A.; Mousavi, S. A. Enhancing $CO_2/N_2$ adsorption selectivity via post-synthetic modification of $NH_2$-UiO-66(Zr). *Microporous Mesoporous Mater.* **2018**, *257*, 193−201.
(22) Huang, A.; Wan, L.; Caro, J. Microwave-assisted synthesis of well-shaped UiO-66-$NH_2$ with high $CO_2$ adsorption capacity. *Mater. Res. Bull.* **2018**, *98*, 308−313.
(23) Xian, S.; Wu, Y.; Wu, J.; Wang, X.; Xiao, J. Enhanced dynamic $CO_2$ adsorption capacity and $CO_2/CH_4$ selectivity on polyethylenimine-impregnated UiO-66. *Ind. Eng. Chem. Res.* **2015**, *54*, 11151−11158.
(24) Li, L. J.; Liao, P. Q.; He, C. T.; Wei, Y. S.; Zhou, H. L.; Lin, J. M.; Li, X. Y.; Zhang, J. P. Grafting alkylamine in UiO-66 by charge-assisted coordination bonds for carbon dioxide capture from high-humidity flue gas. *J. Mater. Chem. A* **2015**, *3*, 21849−21855.
(25) Molavi, H.; Joukani, F. A.; Shojaei, A. Ethylenediamine grafting to functionalized $NH_2$-UiO-66 using green aza-Michael addition reaction to improve $CO_2/CH_4$ adsorption selectivity. *Ind. Eng. Chem. Res.* **2018**, *57*, 7030−7039.
(26) Vahidi, M.; Rashidi, A. M.; Tavasoli, A. Preparation of piperazine-grafted amine-functionalized UiO-66 metal organic framework and its application for $CO_2$ over $CH_4$ separation. *J. Iran. Chem. Soc.* **2017**, *14*, 2247−2253.
(27) Mcdonald, T. M.; Lee, W. R.; Mason, J. A.; Wiers, B. M.; Chang, S. H.; Long, J. R. Capture of carbon dioxide from air and flue gas in the alkylamine-appended metal-organic framework mmen-$Mg_2$(dobpdc). *J. Am. Chem. Soc.* **2012**, *134*, 7056−7065.
(28) Zhang, Z.; Xian, S.; Xia, Q.; Wang, H.; Li, Z.; Li, J. Enhancement of $CO_2$ adsorption and $CO_2/N_2$ selectivity on ZIF-8 via postsynthetic modification. *AIChE J.* **2013**, *59*, 2195−2206.
(29) Huang, X.; Lu, J.; Wang, W.; Wei, X.; Ding, J. Experimental and computational investigation of $CO_2$ capture on amine grafted metal-organic framework $NH_2$-MIL-101. *Appl. Surf. Sci.* **2016**, *371*, 307−313.
(30) Lin, Y.; Yan, Q.; Kong, C.; Chen, L. Polyethyleneimine incorporated metal-organic frameworks adsorbent for highly selective $CO_2$ capture. *Sci. Rep.* **2013**, *3*, No. 1859.
(31) Lin, Y.; Lin, H.; Wang, H.; Suo, Y.; Li, B.; Kong, C.; Chen, L. Enhanced selective $CO_2$ adsorption on polyamine/MIL-101(Cr) composites. *J. Mater. Chem. A* **2014**, *2*, 14658−14665.
(32) Yan, Q.; Lin, Y.; Kong, C.; Chen, L. Remarkable $CO_2/CH_4$ selectivity and $CO_2$ adsorption capacity exhibited by polyamine-decorated metal-organic framework adsorbents. *Chem. Commun.* **2013**, *49*, 6873−6875.
(33) Aarti, A.; Bhadauria, S.; Nanoti, A.; Dasgupta, S.; Divekar, S.; Gupta, P.; Chauhan, R. [$Cu_3$(BTC)$_2$]-polyethyleneimine: an efficient MOF composite for effective $CO_2$ separation. *RSC Adv.* **2016**, *6*, 93003−93009.
(34) Zhang, H.; Goeppert, A.; Olah, G. A.; Prakash, G. K. S. Remarkable effect of moisture on the $CO_2$ adsorption of nano-silica supported linear and branched polyethylenimine. *J. $CO_2$ Util.* **2017**, *19*, 91−99.
(35) Lee, C. H.; Hyeon, D. H.; Jung, H.; Chung, W.; Jo, D. H.; Shin, D. K.; Kim, S. H. Effects of pore structure and PEI impregnation on carbon dioxide adsorption by ZSM-5 zeolites. *J. Ind. Eng. Chem.* **2015**, *23*, 251−256.
(36) Li, K.; Jiang, J.; Tian, S.; Yan, F.; Chen, X. Polyethyleneimine−nano silica composites: a low-cost and promising adsorbent for $CO_2$ capture. *J. Mater. Chem. A* **2015**, *3*, 2166−2175.
(37) Liu, F.; Huang, K.; Yoo, C. J.; Okonkwo, C.; Tao, D. J.; Jones, C. W.; Dai, S. Facilely synthesized meso-macroporous polymer as support of poly(ethyleneimine) for highly efficient and selective capture of $CO_2$. *Chem. Eng. J.* **2017**, *314*, 466−476.
(38) Chavan, S. M.; Shearer, G. C.; Svelle, S.; Olsbye, U.; Bonino, F.; Ethiraj, J.; Lillerud, K. P.; Bordiga, S. Synthesis and characterization of amine-functionalized mixed-ligand metal-organic frameworks of UiO-66 topology. *Inorg. Chem.* **2014**, *53*, 9509−9515.
(39) Ren, J.; Wu, L. B.; Li, B. G. Potential for using simple 1,2,4-triazole salt solutions as highly efficient $CO_2$ absorbents with low reaction enthalpies. *Ind. Eng. Chem. Res.* **2013**, *52*, 8565−8570.
(40) Zhu, J.; Wu, L. B.; Bu, Z.; Jie, S.; Li, B. G. Synthesis and $CO_2$ capture behavior of porous cross-linked polymers containing pendant triazole groups. *Ind. Eng. Chem. Res.* **2017**, *56*, 10155−10163.
(41) Gray, M. L.; Hoffman, J. S.; Hreha, D. C.; Fauth, D. J.; Hedges, S. W.; Champagne, K. J.; Pennline, H. W. Parametric study of solid amine sorbents for the capture of carbon dioxide. *Energy Fuels* **2009**, *23*, 4840−4844.
(42) He, H.; Zhuang, L.; Chen, S.; Liu, H. Solid amine adsorbent prepared by molecular imprinting and its carbon dioxide adsorption properties. *Chem. - Asian J.* **2016**, *11*, 3055−3061.
(43) Devautour-Vinot, S.; Maurin, G.; Serre, C.; Horcajada, P.; Cunha, D. P. D.; Guillerm, V.; Costa, E. D. S.; Taulelle, F.; Martineau, C. Structure and dynamics of the functionalized MOF type UiO-66(Zr): NMR and dielectric relaxation spectroscopies coupled with DFT calculations. *Chem. Mater.* **2012**, *24*, 2168−2177.
(44) Saleem, H.; Rafique, U.; Davies, R. P. Investigations on post-synthetically modified UiO-66-$NH_2$ for the adsorptive removal of heavy metal ions from aqueous solution. *Microporous Mesoporous Mater.* **2016**, *221*, 238−244.
(45) Valenzano, L.; Civalleri, B.; Chavan, S.; Bordiga, S.; Nilsen, M. H.; Jakobsen, S.; Lillerud, K. P.; Lamberti, C. Disclosing the complex structure of UiO-66 metal organic framework: a synergic combination of experiment and theory. *Chem. Mater.* **2011**, *23*, 1700−1718.
(46) Su, X.; Bromberg, L.; Martis, V.; Simeon, F.; Huq, A.; Hatton, T. A. Postsynthetic functionalization of Mg-MOF-74 with tetraethylenepentamine: structural characterization and enhanced $CO_2$ adsorption. *ACS Appl. Mater. Interfaces* **2017**, *9*, 11299−11306.
(47) Samanta, A.; Zhao, A.; Shimizu, G. K. H.; Sarkar, P.; Gupta, R. Post-combustion $CO_2$ capture using solid sorbents: a review. *Ind. Eng. Chem. Res.* **2012**, *51*, 1438−1463.
(48) Ren, J.; Wu, L. B.; Li, B. G. Preparation and $CO_2$ sorption/desorption of N-(3-aminopropyl)aminoethyl tributylphosphonium amino acid salt ionic liquids supported into porous silica particles. *Ind. Eng. Chem. Res.* **2012**, *51*, 7901−7909.
(49) Liu, Z.; Du, Z.; Zou, W.; Mi, J.; Li, H.; Wang, Y.; Zhang, C. Moisture-resistant porous polymer from concentrated emulsion as low-cost and high-capacity sorbent for $CO_2$ capture. *RSC Adv.* **2013**, *3*, 18849−18856.
(50) Han, J.; Du, Z.; Zou, W.; Li, H.; Zhang, C. Moisture-responsive hydrogel impregnated in porous polymer foam as $CO_2$ adsorbent in high-humidity flue gas. *Ind. Eng. Chem. Res.* **2015**, *54*, 7623−7631.
(51) Wu, Y.; Wang, J.; Muhammad, Y.; Subhan, S.; Zhang, Y.; Ling, Y.; Li, J.; Zhao, Z.; Zhao, Z. Pyrrolic N-enriched carbon fabricated from dopamine-melamine via fast mechanochemical copolymerization for highly selective separation of $CO_2$ from $CO_2/N_2$. *Chem. Eng. J.* **2018**, *349*, 92−100.
(52) McCann, N.; Maeder, M.; Attalla, M. Simulation of enthalpy and capacity of $CO_2$ absorption by aqueous amine systems. *Ind. Eng. Chem. Res.* **2008**, *47*, 2002−2009.
(53) Gupta, M.; da Silva, E. F.; Hartono, A.; Svendsen, H. F. Theoretical study of differential enthalpy of absorption of $CO_2$ with MEA and MDEA as a function of temperature. *J. Phys. Chem. B* **2013**, *117*, 9457−9468.


DOI: 10.1021/acsomega.8b02319
*ACS Omega* 2019, 4, 3188−3197

(54) Ebune, G. E. Carbon Dioxide Capture from Power Plant Flue Gas Using Regenerable Activated Carbon Powder Impregnated with Potassium Carbonate. M.S. Thesis, 2008.
(55) DeCoste, J. B.; Peterson, G. W.; Jasuja, H.; Glover, T. G.; Huang, Y.-g.; Walton, K. S. Stability and degradation mechanisms of metal−organic frameworks containing the $Zr_6O_4(OH)_4$ secondary building unit. *J. Mater. Chem. A* **2013**, *1*, 5642−5650.
(56) Goeppert, A.; Czaun, M.; May, R. B.; Prakash, G. K.; Olah, G. A.; Narayanan, S. R. Carbon dioxide capture from the air using a polyamine based regenerable solid adsorbent. *J. Am. Chem. Soc.* **2011**, *133*, 20164−20167.



DOI: 10.1021/acsomega.8b02319
*ACS Omega* 2019, 4, 3188−3197